IEEE Access
Multidisciplinary | Rapid Review | Open Access Journal

Received April 3, 2018, accepted May 1, 2018, date of publication May 8, 2018, date of current version June 5, 2018.

Digital Object Identifier 10.1109/ACCESS.2018.2834470

Robust GPS Carrier Tracking Model Using Unscented Kalman Filter for a Dynamic Vehicular Communication Channel

JIACHEN YIN, RAJESH TIWARI, (Member, IEEE), AND MARTIN JOHNSTON, (Member, IEEE)
School of Engineering, Newcastle University, Newcastle upon Tyne NE1 7RU, U.K.

Corresponding author: Jiachen Yin (j.yin3@ncl.ac.uk)

This work was supported by the Engineering and Physical Science Research Council under Grant EP/H004637/1.

ABSTRACT The carrier tracking loop in a GPS receiver is considered to be an important process but also a weak link since the loss of signal lock can occur in a variety of situations. Low carrier-to-noise ratios and highly dynamic environments are common scenarios for a vehicular communication channel when random phase fluctuations in a dynamic environment are common. We propose a novel and robust carrier tracking approach by dynamically integrating an adaptive unscented Kalman filter assisted by a third-order phase lock loop in order to improve the robustness of tracking capability and accuracy in dense and dynamic environments. Experiments are conducted to investigate the tracking performance of the proposed carrier tracking approach and compare it with existing algorithms for generic GPS receiver. Results indicate that the proposed approach has a better performance in tracking capability and tracking accuracy in highly dynamic environments, and the proposed method achieves a better performance on vehicular communication channels.

INDEX TERMS Phase lock loop, unscented Kalman filter, software-based GPS receiver, decentralized information sharing.

I. INTRODUCTION

In vehicle-to-vehicle (V2V) communication, consistent and continuous vehicular positioning and continuous tracking of GPS seconds (timing) for synchronization between vehicles or infrastructure in a vehicular network under any circumstance is required to avoid collisions and provide navigation services, particularly for autonomous or semi-autonomous vehicles operating under harsh and highly dynamic environments. The GPS is a fully operated satellite-based system that can provide position, velocity and time. However, the availability of the GPS service is highly dependent on the carrier signal successfully locking. A third-order phase lock loop (PLL) is the recommended carrier lock loop because of its superior noise rejection and lower steady-state error, however the performance of a conventional third-order PLL is restricted by the tracking bandwidth and its phase discriminating capability [1]. Furthermore, the trade off between tracking bandwidth and tracking accuracy cannot be neglected. On a vehicular communication channel, greater tracking bandwidth is required in order to maintain the lock in harsh environments due to Doppler shift, however greater tracking bandwidth can increase the noise level in the tracking loop.

Due to the aforementioned requirement, aided carrier tracking approaches have been proposed such as the implementation of a Kalman filter (KF), extended Kalman filter (EKF) or unscented Kalman filter (UKF)-based carrier tracking loops in order to improve the carrier phase tracking ability [2]–[6]. An analysis of the performance of a Kalman filter-based carrier tracking loops in [7] indicates that all of these Kalman filter-based carrier tracking schemes are restricted by prior knowledge that may not match with next-generation vehicular communication channels, which is very dynamic and varying with within the urban and rural region. Furthermore, some prior information is rarely predefined and these mismatches could cause a degradation of tracking performance. Thus, an adaptive KF that could recursively estimate the noise covariance has been proposed in order to mitigate the prior information matching challenge [8]. However, the adaptive KF based scheme is restricted by its linear model. The adaptive EKF based scheme improved on this by eliminating the need for the linear model, but its

Jacobian matrix carries a large computational cost. The adaptive UKF-based scheme, which uses the unscented transform to linearize a nonlinear model, is more efficient and accurate compared to the adaptive EKF. However, as a quasi open loop, the adaptive UKF-based carrier tracking loop has a higher noise level compare to a closed loop.

Therefore, we propose a novel and robust carrier tracking method by dynamically integrating an adaptive UKF and third-order PLL using a decentralized information sharing technique. The two tracking loops work independently and cooperatively since the adaptive UKF and third-order PLL can each track the carrier signal individually. Tracking results from each loop are integrated by calculated weights in order to obtain a final optimal tracking result.

Field experiments on University premises were conducted for the case of a highly dense and dynamic channel comprising multipath signals in an urban environment. A Universal Software Radio Peripheral (USRP) used for the collection of GPS L1 band which is post-processed using in-home GPS software receiver. The tracking performance is mainly compared against adaptive KF based phase lock loop [2] which is widely use in generic GPS receivers. with different tracking bandwidths.

The remainder of this paper is organized as follows: section II reviews the GPS L1 band signal structure and unscented Kalman filter and then elaborates on the proposed tracking algorithm and implementation. Section III introduces the experiment and analyses the results. The conclusion is presented in Section IV.

II. CARRIER TRACKING ALGORITHM AND IMPLEMENTATION

A generic incoming GPS signal $u_i(t)$ can be expressed in the time domain as

$$u_i(t) = A \times D(t) \times C(t-\tau)\cos[(\omega_c + \omega_d)t + \phi_i] + n(t), \tag{1}$$

where A is the signal amplitude, $D(t)$ is the navigation data bit, $C(t)$ is the spreading C/A code, τ is the code delay of the received signal, ω_c is the incoming carrier frequency, ω_d is Doppler frequency shift, ϕ_i is the carrier phase in radians and $n(t)$ is the noise. The aim of the carrier tracking loop is to continuously lock carrier parameters, such as the frequency and phase of the incoming signal, in order to retrieve the navigation data frame, GPS timing and estimation of the precise range between satellite and receiver for positioning. The proposed carrier tracking approach is discussed in the following section.

A. UNSCENTED TRANSFORM

For a nonlinear function, it is intuitively easier to approximate its distribution rather than its arbitrary nonlinear function [9]. The unscented transform (UT) uses the calculated mean and variance of a random variable to propagate through a nonlinear function [10] which is the conventional case for receiving random phase fluctuations in the carrier tracking loop.

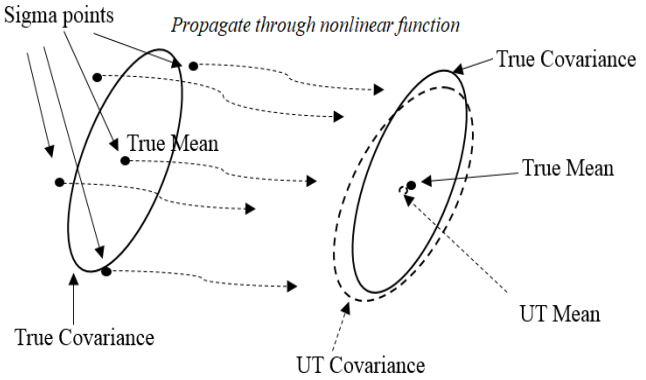

FIGURE 1. Procedure of unscented transform.

In order to have a transformation as in Fig.1, sigma points which are selected via the mean and variance capture the high order information of the distribution as expressed in the solid circle. Through the nonlinear propagation the accuracy of the approximation can achieve up to the 2nd order (Taylor series expansion) of nonlinearity as expressed in the dash circle [11]. A random variable x with L dimensions has mean $\bar{x}$ and covariance P_x presented as (2).

$$\begin{aligned} \bar{x} &= E[x] \\ P_x &= E[(x-\bar{x}_0)(x-\bar{x}_0)^T] \end{aligned} \tag{2}$$

A matrix X with L dimensions needs 2L+1 sigma vectors X_i to form its distribution, which are:

$$\begin{aligned} X_i &= \bar{x}; \quad for\ i = 0 \\ X_i &= \bar{x} + (\sqrt{(L+\lambda)P_x})_i; \quad for\ i = 1, ..., L \\ X_i &= \bar{x} + (\sqrt{(L+\lambda)P_x})_i; \quad for\ i = L+1, ..., 2L \end{aligned} \tag{3}$$

where λ is a scaling parameter and can be obtained by $\lambda = \alpha^2(L+\kappa) - L$, α decides the spread of the sigma points around $\bar{x}$ and is usually a small positive value (0.001) and κ is another scaling parameter that is normally set to zero [12]. After Propagating the sigma vectors X_i through the nonlinear function $f(x)$ we obtain

$$y_i = f(X_i); \quad i = 0, ..., 2L. \tag{4}$$

The mean and covariance of the transformed output y_i can be obtained by a weighted mean and covariance as (5) [11]:

$$\begin{aligned} \bar{y} &= \sum_{i=0}^{2L} W_i^m y_i \\ P_y &= \sum_{i=0}^{2L} W_i^c [(y_i - \bar{y})(y_i - \bar{y})^T] \end{aligned} \tag{5}$$

The above weights can be calculated using (6) [11]

$$\begin{aligned} W_i^m &= \lambda/(L+\lambda) \quad i = 0 \\ W_i^c &= \lambda/(L+\lambda) + (1+\alpha^2+\beta) \quad i = 0 \\ W_i^m &= W_i^c = 1/2(L+\lambda) \quad i = 1, ...2L \end{aligned} \tag{6}$$

where β is equal to 2 [11] and we consider our model to have a Gaussian distribution as studied in [13].

B. ADAPTIVE UNSCENTED KALMAN FILTER AND IMPLEMENTATION

The unscented Kalman filter is based on an expansion of the unscented transform. In the carrier tracking loop, the unscented Kalman filter can track the carrier signal phase directly instead of the phase error [6].

$$\Phi = \phi_c + \Delta t\omega_d + \frac{\Delta t^2}{2}\omega_a + \frac{\Delta t^3}{6}\omega_j \tag{7}$$

$$\vec{x}_t = A\vec{x}_{t-1} + \Delta t\omega_{nco} + noise \tag{8a}$$

$$\begin{bmatrix}\phi_c\\ \omega_d\\ \omega_a\\ \omega_j\end{bmatrix}_t = \begin{bmatrix}1 & \Delta t & \frac{\Delta t^2}{2} & \frac{\Delta t^3}{6}\\ 0 & 1 & \Delta t & \frac{\Delta t^2}{2}\\ 0 & 0 & 1 & \Delta t\\ 0 & 0 & 0 & 1\end{bmatrix}\begin{bmatrix}\phi_c\\ \omega_d\\ \omega_a\\ \omega_j\end{bmatrix}_{t-1} + \Delta t\omega_{NCO} + diag\,(W_t) \tag{8b}$$

$$A = \begin{bmatrix}1 & \Delta t & \frac{\Delta t^2}{2} & \frac{\Delta t^3}{6}\\ 0 & 1 & \Delta t & \frac{\Delta t^2}{2}\\ 0 & 0 & 1 & \Delta t\\ 0 & 0 & 0 & 1\end{bmatrix} \tag{8c}$$

The incoming carrier signal phase Φ can be represented as (8a) and the state model in matrix form can be represented as (8a,8b). The state matrix $\vec{x}$ has four vectors which are $\vec{x} = [\phi_c \quad \omega_d \quad \omega_a \quad \omega_j]^T$, ϕ_e is the carrier phase, ω_d represents the Doppler frequency, ω_a and ω_j are the first and second order of the Doppler frequency change rate. A is the state transition matrix in 8c, Δt is the time interval, ω_{NCO} is the phase shift of the numerical oscillator, W_t represents the processing noise with zero mean and its covariance is denoted as Q, $W_t \sim (0, Q)$. The collected signals using a universal software radio peripheral (USRP) are the I and Q samples after low pass filtering (the block called integration and dump) presented as (9):

$$\begin{aligned} I_{p,t} &= A \times D(t) \times [\cos((\phi_c + \Delta t\omega_d + \frac{\Delta t^2}{2}\omega_a + \frac{\Delta t^3}{6}\omega_j)]\\ Q_{p,t} &= A \times D(t) \times [\sin((\phi_c + \Delta t\omega_d + \frac{\Delta t^2}{2}\omega_a + \frac{\Delta t^3}{6}\omega_j)] \end{aligned} \tag{9}$$

Directly using I_p and Q_p as the measurement matrix vector can cause polarity reversal, thus in order to avoid polarity reversal of the navigation data, I_p and Q_p need to treated as

$$\begin{aligned} I_{p,t}^2 - Q_{p,t}^2 &= A^2 \times D(t)^2 \times \cos(2\Phi)\\ 2I_{p,t} \times Q_{p,t} &= A^2 \times D(t)^2 \times \sin(2\Phi) \end{aligned} \tag{10}$$

where Φ is the phase of carrier signal. The normalized amplitude can be obtained through (11)

$$A_t^2 \cdot D_t^2 = \sum_{i=t-n}^{t} (I_{p,t}^2 + Q_{p,t}^2)/n \tag{11}$$

where n is the coherent integration time. Finally, the measurement matrix z can be represented as

$$\begin{aligned} z = \begin{bmatrix}I_z\\ Q_z\end{bmatrix} &= \begin{bmatrix}I_{p,t}^2 - Q_{p,t}^2\\ 2I_{p,t} \times Qp,t\end{bmatrix} \cdot (\sum_{i=t-n}^{t} (I_{p,t}^2 + Q_{p,t}^2)/n)^{-1}\\ &= \begin{bmatrix}\cos(2\Phi)\\ \sin(2\Phi)\end{bmatrix} + diag(V_t) \end{aligned} \tag{12}$$

where the measurement noise, $V_t \sim (0, R)$, has zero mean and covariance R. Starting from the estimated mean value of the state matrix $E(\hat{x}_{t-1})$ and the variance matrix P_{t-1} at time $t-1$, 9 sigma points ($i = 1, ..., 9$) are selected using (3) since our state matrix $x = [\phi_c \quad \omega_d \quad \omega_a \quad \omega_j]^T$ contains 4 vectors. These 9 points are mathematically expressed as (13.1) and then the covariance matrix $P_{t-1|t-1}$ is updated as in (13.2). Substituting the output $\hat{x}^i_{t|t-1}$ into the measurement model equation $h(\cdot)$ as in (14.1), $h(\cdot)$ is a nonlinear trigonometric function presented in (12). The weighted mean output value with respect to state and measurement models can be calculated as (13.3) and (14.2). These values are used to obtain the covariance matrix $P_{\bar{y}\bar{y}}$ and $P_{\bar{x}\bar{y}}$, which are the covariance of the measurement function approximation and the covariance of the state and measurement function approximation. Prediction stage and measurement stage are presented as (13) and (14).

Prediction stage:

$$\hat{x}^i_{t|t-1} = A \cdot \hat{x}^i_{t-1|t-1} + \Delta t\omega_{nco} \tag{13.1}$$

$$P_{t|t-1} = A \cdot P_{t-1|t-1} \cdot A + Q \tag{13.2}$$

$$\bar{x}_{t|t-1} = \sum_{i=0}^{2L} W_i^m \hat{x}^i_{t|t-1} \tag{13.3}$$

Measurement stage:

$$\gamma_{t|t-1} = h(\hat{x}^i_{t|t-1}) \tag{14.1}$$

$$\bar{y}_{t|t-1} = \sum_{i=0}^{2L} W_i^m \gamma_{t|t-1} \tag{14.2}$$

$$P_{\bar{y}\bar{y}} = \sum_{i=0}^{2L} W_i^c [(\gamma_{i,t|t-1} - \bar{y}_{t|t-1})(\gamma_{i,t|t-1} - \bar{y}_{t|t-1})^T] + R \tag{14.3}$$

$$P_{\bar{x}\bar{y}} = \sum_{i=0}^{2L} W_i^c [(\hat{x}_{i,t|t-1} - \bar{x}_{t|t-1})(\gamma_{i,t|t-1} - \bar{y}_{t|t-1})^T] \tag{14.4}$$

$$K_t = P_{\bar{x}\bar{y}} P_{\bar{y}\bar{y}}^{-1} \tag{14.5}$$

$$P_t = P_{t|t-1} - K_t P_{\bar{y}\bar{y}} K_t^T \tag{14.6}$$

$$\bar{x}_{t|t} = \bar{x}_{t|t-1} + K_t(y_t - \bar{y}_{t|t-1}) \tag{14.7}$$

where $\bar{x}_{t|t}$ is the state matrix which contains optimal mean vectors of the carrier signal parameters at time t and these mean vectors can be used to select sigma points for $t+1$ time estimation.

However, in GPS signal carrier tracking, the processing noise covariance is rarely predefined especially under highly

dynamic environments. The unscented Kalman filter will suffer performance degradation if the prior information is mismatched with the real system. Therefore, in our application, due to the linear processing model, the processing noise covariance Q could be recursively updated using the covariance matching method [14].

In the measurement update process, the covariance of the innovation sequence ξ_t, has proved to be independent of time and is approximated from its sampled covariance [15], as given by (14a-c).

$$\xi_t = y_t - \bar{y}_{t|t-1} \tag{15a}$$

$$C_t \equiv Cov\,(\xi_t) \tag{15b}$$

$$C_t = \frac{1}{N}\sum_{t=k}^{N} \xi_t \xi_{t-k}^T, \tag{15c}$$

where k represents a delay of length k from t and N is the number of samples. In the state processing model, the processing noise w_t can be represented as (16)

$$w_{t-1} = x_t - A(x_{t-1}). \tag{16}$$

The Kalman filter estimation equation (13.11) can be rewritten as (17)

$$x_t - x_{t-1} = K_t(y_t - \bar{y}_{t|t-1}) \tag{17}$$

In our application, x_t and x_{t-1} are represented by their mean values, $\bar{x}_t$ and $\bar{x}_{t-1}$. Therefore, combining (16) and (17)

$$w_{t-1} = \bar{x}_t - \bar{x}_{t-1} = K_t(y_t - \bar{y}_{t|t-1}). \tag{18}$$

To estimate the innovation sequence covariance, the processing noise covariance can be obtained as

$$Q_{t-1} = K_t C_t K_t^T. \tag{19}$$

In a time-invariant system with a high sampling frequency, variation within successive epoch is very small, therefore the successive variation of the Kalman gain element is small enough, thus $K_t \approx K_{t-1}$

$$Q_{t-1} = K_{t-1} C_t K_{t-1}^T. \tag{20}$$

1) DECENTRALIZED INFORMATION SHARING TECHNIQUE

Benefiting from the strong capability of the nonlinear model's tolerance, the unscented Kalman filter could replace the phase discriminator and loop filter to directly track the carrier signal phase. However, as a quasi open loop, an AUKF-based carrier tracking loop could have a higher noise level compared to a closed loop. Therefore, in order to mitigate the noise level in an AUKF-based carrier tracking loop, we implement a conventional third-order phase lock loop using the decentralized information sharing technique. The decentralized information sharing technique is widely used in data fusion applications. The information sharing factor can be obtained by the eigenvalues and eigenvectors of the covariance matrix from each subsystem [16].

In our approach, the adaptive unscented Kalman filter and third-order PLL are considered as two independent subsystems. The covariance matrix P_{AUKF} can be obtained directly from AUKF processing and a standard Kalman filter needs to be implemented to estimate the processing covariance P_{PLL} of the third-order PLL. The covariance matrix of the i_{th} subsystem can be decomposed as

$$P_i = \ell \Lambda_i \ell^T, \tag{21}$$

where $\Lambda_i = diag\,\{\lambda_{i1}, \lambda_{i2}, ..., \lambda_{in}\}$, $\lambda_{i1}....\lambda_{in}$ is the eigenvalue of P_i. In order to avoid negative values of λ, ℓ, the eigenvector of P, can be replaced by $P_i^T P_i$ therefore

$$P_i^T P_i = \ell' \Lambda_i'(\ell'^T) \tag{22}$$

where $\Lambda_i' = diag\left\{\lambda_{i1}^2, \lambda_{i2}^2, ..., \lambda_{in}^2\right\}$. The information sharing factor β_i can be expressed as

$$\beta_i = \frac{1}{N-1}\frac{\sum_{j=1}^{N} tr\Lambda_j - tr\lambda_i}{\sum_{j=1}^{N} tr\Lambda_j} \tag{23}$$

where N is the number of subsystems and $j = 1, 2, 3, ..., N$. A greater value of β_i relates to a more stable estimated subsystem that will take more weight on information sharing and have a larger impact on the entire system. The integrated carrier tracking scheme in Fig.2 demonstrated two subsystems. The adaptive unscented Kalman filter algorithm that recursively estimates the processing noise covariance can track the incoming carrier signal in parallel with a third-order PLL and integrate the results using the information sharing factors. The performance will be discussed in detail in the following section.

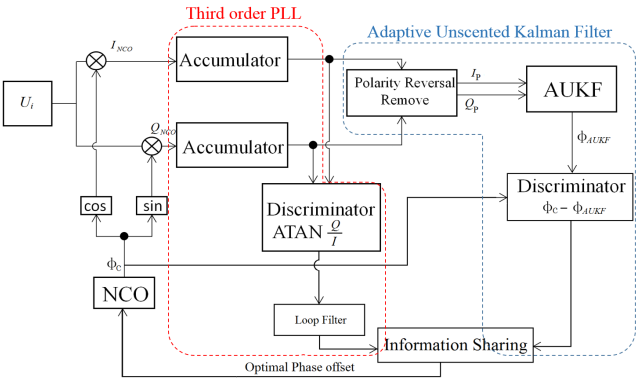

FIGURE 2. Procedure diagram of the proposed approach.

III. EXPERIMENT RESULTS AND ANALYSIS

As previously mentioned, a study in [2] has compared the performance between a KF-based phase lock loop and conventional phase lock loop. Several advantages have been discussed, however the comparison is simulation-based and the noise covariance is predefined. In this section we conduct a field experiment in order to compare and analyze the tracking results from the adaptive Kalman filter-based PLL and the proposed dynamic integration tracking scheme.

FIGURE 3. Experiment setup.

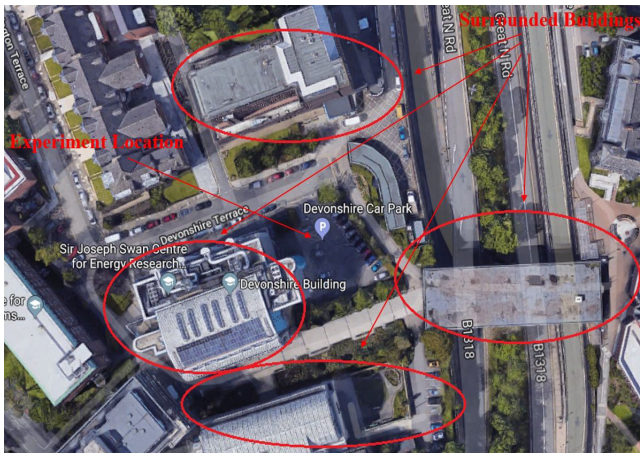

FIGURE 4. Experiment location.

A. EXPERIMENT LOCATION AND SETUP

The experiment is illustrated in Fig.3 and Fig.4 conducted at the Devonshire Building car park, Newcastle University, UK since the location is surrounded by buildings and the open park area is convenient for maneuvering a trolley. The experiment was undertaken for 3 consecutive days. A USRP (2^{nd} component in the figure) and a Leica AX1203+ GNSS antenna (1^{st} component in the figure) works as a front-end, the received center frequency is 1575.42 MHz corresponding to the L1 band. The RF signal is down-converted to a baseband signal by the USRP and is then sampled at 5MHz. The recorded data type is a 16 bit integer, which is the only option available from the USRP. However, 16-bit data types are not suitable due to the high volume of data received so we have converted the data into 8-bit integers. The baseband signal is then up-converted to an IF band at 2.5 MHz without any loss of signal characteristic and up-sampled at rate of 10 MHz. As an active GNSS antenna, Leica AX1203+ needs to be powered by a PP3 battery through a bias tee (5^{th} and 6^{th} component in the figure). A precise atomic clock Symmetricom CSAC SA.45s (3^{rd} component in the figure) is used to provide a 10 MHz external clock source since the USRP uses a generic (TXCO) oscillator [17] and is not suitable for a highly dynamic environment. In order to simulate a non-stationary environment, all devices are powered by two 12V batteries (7^{th} component in figure). As mentioned before, the performance of the tracking loop is limited by the tracking bandwidth, since greater tracking bandwidth can degrade the performance. Therefore, the experiment requires two tracking bandwidths to be set for performance comparison.

B. RESULTS AND DISCUSSION

Starting from a modified serial searching acquisition approach [18], the tracking bandwidth is set to 12 Hz, which is a relatively large bandwidth for a third-order PLL. As can be seen in Fig.5, both tracking approaches can lock the carrier signal successfully in general, but it can also be seen that the proposed method outperforms the AKF-based approach overall.

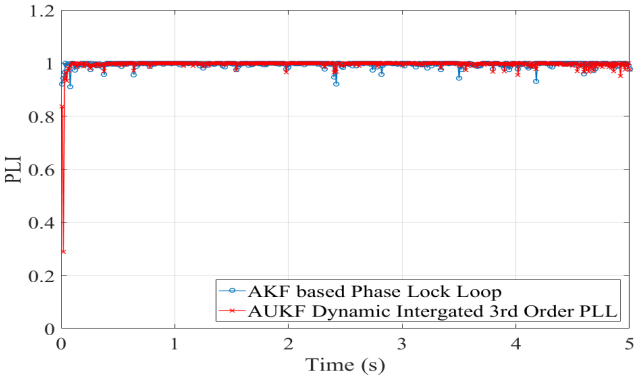

FIGURE 5. Phase lock indicator comparison at bandwidth 12 Hz.

Due to the binary phase shift keying (BPSK) modulation used in GPS signals, the demodulated constellation map of the I and Q components are presented as Fig.6. In an ideal constellation map of BPSK, all the points have a constant value in the I component and 0 value in the Q component. In Fig.6, all approaches can successfully demodulate both the I and Q components, however the Q component in the proposed method has a smaller variation compared to the AKF based PLL, which means the noise level from the proposed method is lower than the AKF based PLL. This can also be proved in Fig.7, where the output of the phase discriminator from the proposed approach is smaller than the AKF-based PLL. The phase variances from these two approaches are presented as Fig.8. The phase variance from the AKF-based PLL approach is on average 1.5 however the phase variance of the proposed AUKF dynamically integrated 3_{rd} order PLL method has an average less than 1.

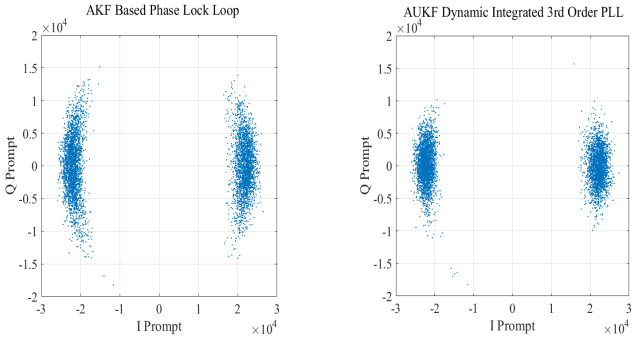

FIGURE 6. Processed I and Q at bandwidth 12 Hz.

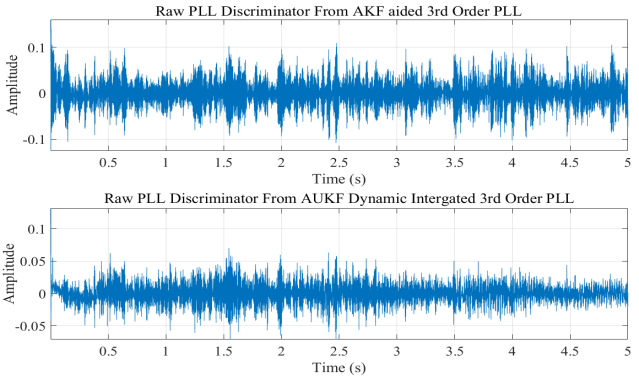

FIGURE 7. Phase difference at bandwidth 12 Hz.

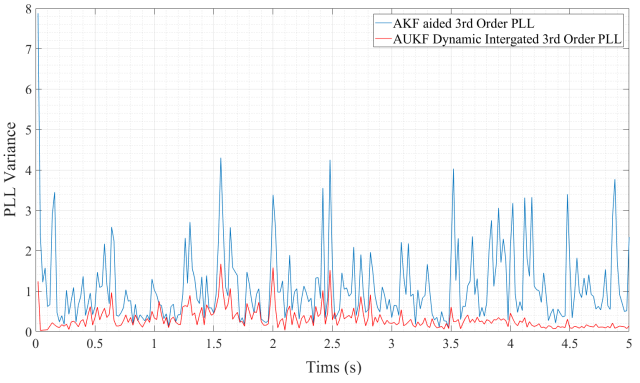

FIGURE 8. Phase variance comparison at bandwidth 12 Hz.

Within the proposed carrier tracking approach, the sharing factor decides the sharing weight between the adaptive unscented Kalman filter and the third order PLL. The sum of all sharing factors β is equal to 1 as mentioned previously. As Fig.9 demonstrated, at the very beginning the sharing factor from the third order PLL β_1 is very high and the third order PLL dominates the entire loop because the adaptive unscented Kalman filter needs to recursively estimate the covariance and reach a steady state. Then the sharing factor of the AUKF-based subsystem β_2 increases dramatically and starts to dominate the carrier tracking loop. Once the noise level reduces to a relevant level, β_2 tends to decrease and the tracking loop will be handed over to the third-order PLL.

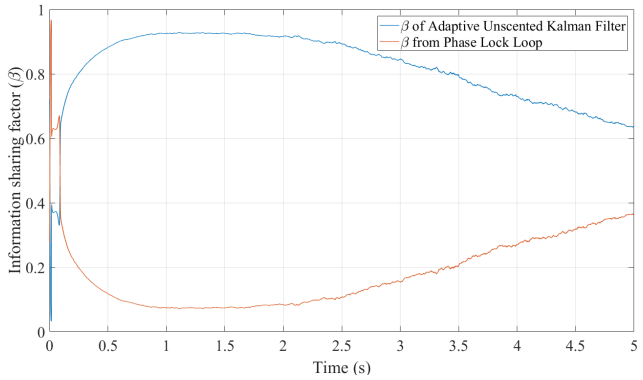

FIGURE 9. Decentralized information sharing factors (β) at bandwidth 12 Hz.

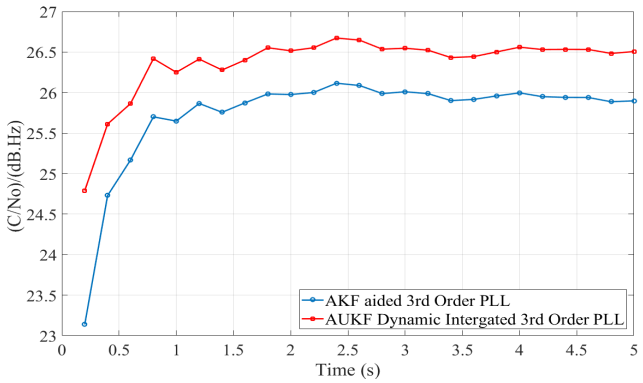

FIGURE 10. Carrier to noise ratio comparison at bandwidth 12 Hz.

Carrier-to-noise ratio (C/N_o) is an important parameter for describing GPS receiver performance, where a higher C/N_o indicates a better phase estimation and location determination. The C/N_o estimation in this experiment uses the Narrowband-Wideband power ratio method [19]. Comparing (C/N_o) within these two methods, the proposed method shows an improvement of 1.5 dB at the beginning, and 1 dB on average. The proposed approach does not show a significant improvement due of the relatively low tracking bandwidth.

The tracking bandwidth was increased to 13 Hz in order to increase the tracking range and improve the dynamic tracking capability. As Fig.11 presented, the AKF-based PLL has difficulty in locking the incoming signal phase and eventually loses the lock, yet the proposed adaptive unscented Kalman filter dynamically integrated third-order PLL can still retain the lock. As Fig.12 demonstrates, the constellation map for the AKF-based PLL struggles to distinguish the I and Q components because of the high noise level, however, the proposed tracking approach can still distinguish I and Q components clearly.

The output of the phase discriminator and phase variance are presented in Fig.13 and Fig.14 respectively. Under a larger tracking bandwidth, the AKF based PLL contains a relatively higher noise level, the high noise level from the output of

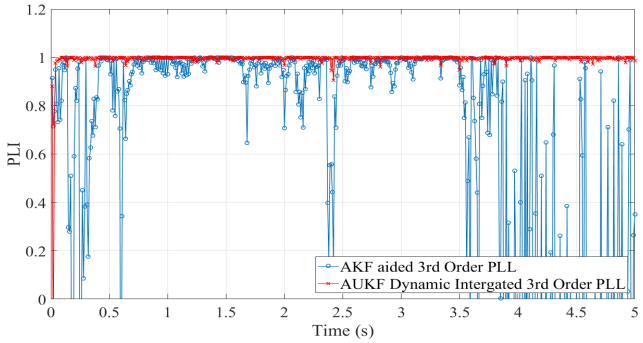

FIGURE 11. Phase lock Loop Indicator Comparison at Bandwidth 13 Hz.

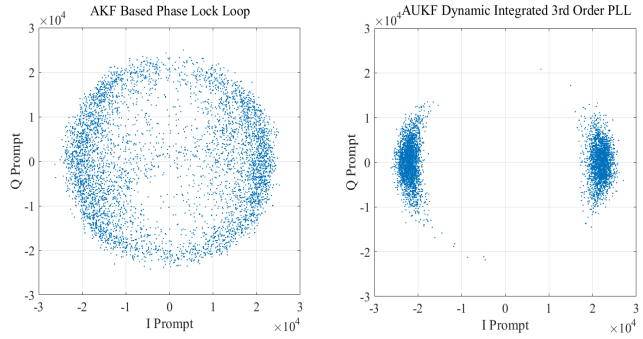

FIGURE 12. Processed I and Q at Bandwidth 13 Hz.

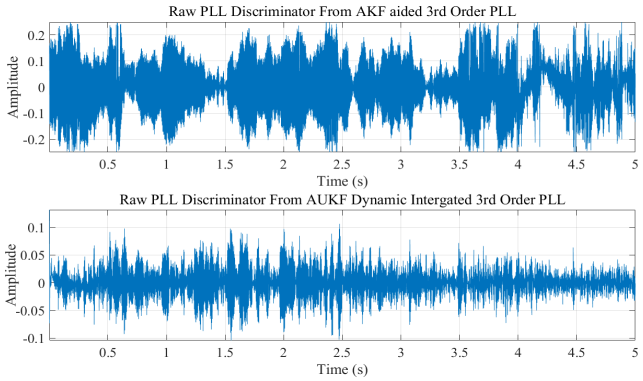

FIGURE 13. Phase difference comparison at bandwidth 13 Hz.

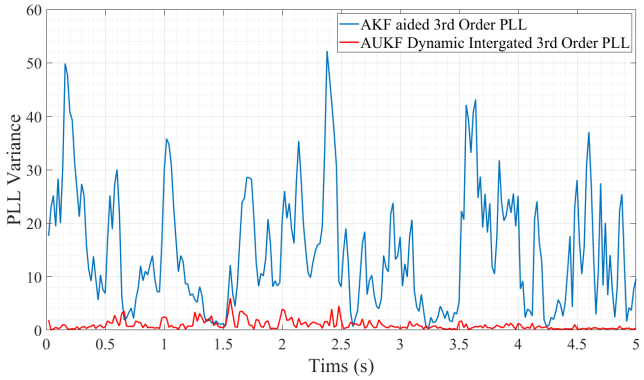

FIGURE 14. Phase variance comparison at bandwidth 13 Hz.

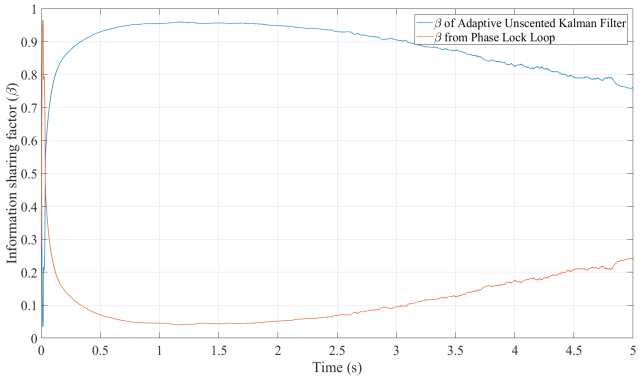

FIGURE 15. Decentralized Information Sharing Factors (β) at Bandwidth 13 Hz.

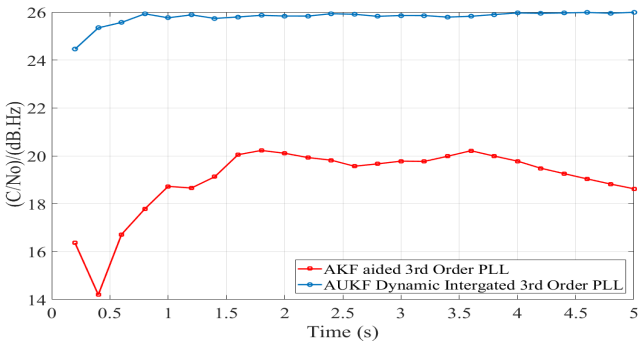

FIGURE 16. Carrier to noise ratio comparison at bandwidth 13 Hz.

the phase discriminator makes the AKF-based PLL carrier tracking loop unstable. However, the proposed approach has significantly better performance compared to the AKF-based PLL approach because of the dynamic integration structure. The information sharing factors are present in Fig.15.

Comparing Fig.15 to Fig.9, the overalltrends are similar, which proves the third-order PLL is more sensitive in this integrated system. However, the AUKF-based tracking loop is more robust and this explains why β_2 dominates the integrated system at most times. Furthermore, it is clear to see that the sharing factor in the AUKF-based tracking loop β_2 has a decreasing trend for both 12 Hz and 13 Hz tracking bandwidths, but the decreasing rate of β_2 under 13 Hz is lower than 12 Hz, which means under a greater tracking bandwidth or higher noise level scenario, the AUKF tracking loop needs a longer time to process in order to track Doppler shift parameters and reduce the noise level.

Unlike 12 Hz, under a 13 Hz tracking bandwidth the proposed approach has a significant improvement compared to the AKF-based PLL, C/N_o has been improved 6 dB on average as Fig.16 illustrates. Comparing Fig.16 to Fig.10, C/N_o from the AKF based PLL has dropped by up to 7 dB due to the increased tracking bandwidth, however this does not affect the proposed approach significantly. The proposed approach exhibits a strong capability to maintain the C/N_o. As shown in Fig.17, the navigation message from the

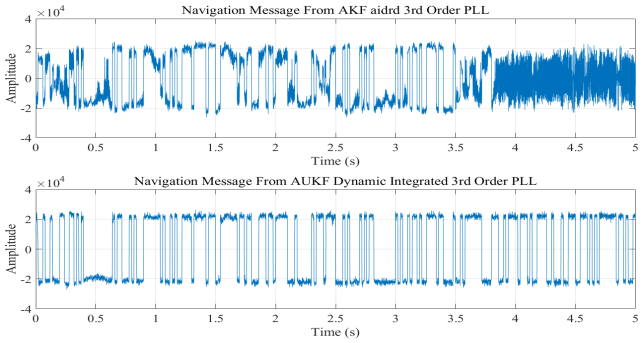

FIGURE 17. Navigation bits at bandwidth 13 Hz.

AKF-based PLL contains a higher level of noise and eventually loses the lock as in Fig.11. In contrast, the proposed approach can still demodulate the navigation message successfully.

IV. CONCLUSION

A novel GPS carrier tracking model using dynamic integration from an adaptive unscented Kalman filter and third-order phase lock loop has been presented in this paper. Experimental results show that the proposed approach can improve the carrier tracking capability. The carrier tracking trade-off issue between tracking bandwidth and accuracy has been tackled using the proposed approach and the field test confirms it can achieve a greater tracking range and still maintain high accuracy. Comparison results indicate that the proposed approach is more stable and robust with respect to phase variance and phase discriminator output. Phase variance comparison results show that the proposed approach has a better steady-state response. Moreover, the phase discriminator output comparison results indicate that the proposed approach has a better noise rejection ability. This can also be proved in the C/N_o comparison.

In vehicular communication, greater tracking bandwidth is essential for the GPS carrier tracking loop since highly dynamic environments are a common occurrence. A greater tracking range and noise-tolerant carrier tracking loop is required for the emerging vehicular communication market. Benefiting from the proposed tracking approach, GPS receivers will be able to fulfill the highly dynamic requirements and retain continuous and consistent positioning results.

ACKNOWLEDGMENT

The authors are grateful to the Nottingham Scientific Ltd., for access to the atomic clock for their experiment.

REFERENCES

[1] E. Kaplan and C. Hegarty, *Understanding GPS: Principles and Applications*. Norwood, MA, USA: Artech House, 2005.

[2] X. Niu, B. Li, N. I. Ziedan, W. Guo, and J. Liu, "Analytical and simulation-based comparison between traditional and Kalman filter-based phase-locked loops," *GPS Solution*, vol. 1, no. 21, pp. 123–135, 2016.

[3] M. L. Psiaki, "Attitude sensing using a global-positioning-system antenna on a turntable," *J. Guid., Control, Dyn.*, vol. 24, no. 3, pp. 474–481, 2001.

[4] N. I. Ziedan and J. L. Garrison, "Extended Kalman filter-based tracking of weak GPS signals under high dynamic conditions," in *Proc. ION GNSS*, 2004, pp. 20–31.

[5] M. L. Psiaki, "Smoother-based GPS signal tracking in a software receiver," in *Proc. ION GPS*, 2001, pp. 2900–2913.

[6] S. Han, W. Wang, X. Chen, and W. Meng, "Design and capability analyze of high dynamic carrier tracking loop based on ukf," in *Proc. 23rd Int. Tech. Meeting Satellite Division Inst. Navigat. (ION GNSS)*, 2001, pp. 1960–1966.

[7] R. Jiang, K. Wang, S. Liu, and Y. Li, "Performance analysis of a Kalman filter carrier phase tracking loop," *GPS Solutions*, vol. 2, no. 21, pp. 551–559, 2016.

[8] K.-H. Kim, G.-I. Jee, and J.-H. Song, "Carrier tracking loop using the adaptive two-stage Kalman filter for high dynamic situations," *Int. J. Control, Autom., Syst.*, vol. 6, no. 6, pp. 948–953, 2008.

[9] J. K. Uhlmann, "Simultaneous map building and localization for real time applications," Univ. of Oxford, Oxford, U.K., Tech. Rep., 1994.

[10] S. J. Julier and J. K. Uhlmann, "New extension of the Kalman filter to nonlinear systems," *Proc. SPIE*, vol. 3068, pp. 182–194, Jul. 1997.

[11] E. A. Wan and R. Van Der Merwe, "The unscented Kalman filter for nonlinear estimation," in *Proc. Adapt. Syst. Signal Process., Commun., Control Symp. (AS-SPCC)*, Oct. 2000, pp. 153–158.

[12] S. J. Julier, J. K. Uhlmann, and H. F. Durrant-Whyte, "A new approach for filtering nonlinear systems," in *Proc. Amer. Control Conf.*, vol. 3. Jun. 1995, pp. 1628–1632.

[13] M. L. Psiaki and H. Jung, "Extended Kalman filter methods for tracking weak GPS signals," in *Proc. ION GPS 15th Int. Tech. Meeting Satellite Division Inst. Navigat.*, 2002, pp. 2539–2553.

[14] R. K. Mehra, "Approaches to adaptive filtering," *IEEE Trans. Autom. Control*, vol. AC-17, no. 5, pp. 693–698, Oct. 1972.

[15] R. K. Mehra, "On the identification of variances and adaptive Kalman filtering," *IEEE Trans. Autom. Control*, vol. AC-15, no. 2, pp. 175–184, Apr. 1970.

[16] N. A. Carlson, "Federated filter for fault-tolerant integrated navigation systems," in *Proc. 21st Century Position Location Navigat. Symp. Rec. Navigat. (IEEE PLANS)*, Nov. 1988, pp. 110–119.

[17] R. Tiwari, H. Strangeways, and S. Skone, "Modeling the effects of ionospheric scintillation on GPS carrier phase tracking using high rate TEC data," in *Proc. 26th Int. Tech. Meeting Satellite Division Inst. Navigat. (ION GNSS)*, Nashville, TN, USA, 2013, pp. 2480–2488.

[18] J. Yin, R. Tiwari, and M. Johnston, "Low-cost dual polarized GPS antenna for effective signal acquisition in multipath environment," in *Proc. Eur. Navigat. Conf. (ENC)*, May 2017, pp. 359–365.

[19] B. W. Parkinson, *Global Positioning System: Theory and Applications*, vol. 1. Washington, DC, USA: AIAA, 1996.

JIACHEN YIN received the B.S. degree in telecommunication science from Assumption University, Thailand, in 2012, and the M.Sc. degree in communications and signal processing from Newcastle University, U.K., in 2015, where he is currently pursuing the Ph.D. degree with the School of Engineering. His research interests include GNSS precise positioning, carrier tracking, and GNSS/INS/LiDAR multi sensor data fusion.

RAJESH TIWARI received the Ph.D. degree. He is currently a Teaching Fellow with the School of Engineering, Newcastle University, U.K. He has background research in Global Navigation Satellite System (GNSS), channel modeling, wireless location and GNSS software receiver designing, and remote sensing. His research interests also include space weather effect on GPS. He participated as a Scientist in the XXVI Indian Scientific Expedition to Antarctica.

In Antarctica, he studied the effect of Aurora on GPS receiver and also did several experiments in marine navigation using GPS receiver, the results published in a book *Antarctica: The Most Interactive Ice Air-Ocean Environment*. He published 15 journal papers, and he was a PI of the EPSRC IAA KTS Project. He received various prestigious awards over the period: the Young Scientist Award, Indian Science Congress, Bhopal Chapter, India; and the Young Scientist Award, International Union of Radio Science, in 2011.

MARTIN JOHNSTON received the B.Sc. degree (Hons.) in physics with electronics from Birmingham University, U.K., in 1999, the M.Sc. degree in electronic engineering from Staffordshire University, U.K., in 2001, and the Ph.D. degree from Newcastle University, U.K., in 2006. From 2006 to 2014, he was a Research Associate with the School of Engineering, Newcastle University, where he is currently a Lecturer. His research interests include the design of advanced error-correcting schemes and low-complexity decoding algorithms, vehicle-to-vehicle communications, and physical-layer security.